We A03

Fall-Off Test Analysis and Transient Pressure Behavior in Foam Flooding

N. Khoshnevis Gargar* (Delft University of Technology), H. Mahani (Shell Global Solutions International, the Netherlands), J.G. Rehling (Shell Global Solutions International, The Netherlands), S. Vincent-Bonnieu (Shell Global Solutions International, The Netherlands), N. Idah Kechut (Petronas Research Sdn. Bhd.) & R. Farajzadeh (Shell Global Solutions International, Delft University of Technology)

SUMMARY

Gas injection projects often suffer from poor volumetric sweep because under reservoir conditions the density and viscosity differences between the gas and the in-situ oil leads to override and bypassing of much of the oil in place. Foam has been suggested as a potential solution to this shortcoming and has shown success in some of the field applications. In the field scale foam can reduce the gas mobility, fight against gravity by inducing excess viscous forces and reduce the gas-oil ratio in the producer. Nevertheless, foam propagation in the reservoir, with low fluid velocities, and survival of foam in the path from injector to producer are among major uncertainties in foam projects. This necessitates the design of surveillance plans to monitor foam rheology and its propagation in porous media.

Usually foam generation inside a porous medium is indirectly inferred from the pressure response; once foam is generated in the reservoir the pressure increases. Foam frequently exhibits non-Newtonian (shear-thinning) behaviour, as it is propagated through the porous medium, which can influence the pressure transient test behaviour. This paper studies different well testing interpretation and pressure behaviour of foam flow in a homogenous reservoir. Local-equilibrium or implicit-texture foam model (that of STARS) are used to model the foam behaviour in porous media.

Pressure fall-off test behaviour presented in this paper is new for foam injection. The flow regimes including inclined radial flow, radial flow, transient section, and reservoir boundary are discussed. A method which uses a pressure and a pressure derivative plot is developed for foam injection so that the mobility changes, flow behaviour index, location of foam front, reservoir parameters and reservoir boundary can be estimated.

The results of this study can be used to analyse data from injection well, where monitoring of the generation, stability and distribution of foam is a key factor in the success of a foam field project. This paper discuss the dependency of the results on foam-model parameters, which indicates that by using pressure transient data one can obtain the foam model parameter.

Introduction

Gas injection is an ideal enhanced oil recovery (EOR) agent: it has high displacement (or microscopic sweep) efficiency and can be injected at very high rates with no major injectivity issue. However, reservoir heterogeneity, viscosity difference between the injected gas and the displaced oil and water, and gravity override of the gas lead to poor macroscopic or volumetric sweep efficiency of gas, bypassing most of the oil in-place and resulting in premature breakthrough of the gas. These problems can be potentially overcome by injecting foam (Andrianov *et al*., 2012; Falls *et al*., 1988; Hirasaki, 1989; Hirasaki and Lawson, 1985; Rossen, 1996; Schramm, 1994; Simjoo *et al*., 2013; Wellington and Vinegar, 1988).

In porous media, gas is dispersed in liquid causing the gas phase to become discontinuous by thin liquid films named lamellae (Falls *et al*., 1988; Hirasaki, 1989; Kovscek and Radke, 1994). The aim is to control the gas mobility by creating lamellae (foam films) along the gas flow paths in the pores.

Foam improves the oil recovery (Chen *et al*., 2013; Farajzadeh *et al*., 2012; Li *et al*., 2010; Ren *et al*., 2011) by

a) providing more favourable mobility control to the gas,
b) reducing the non-uniformities of the displacement front due to heterogeneities of the rock,
c) reducing the excessive gas production which is partially a result of delay in the gas breakthrough, and
d) improving the volumetric sweep efficiency.

Several foam-injection pilots have been conducted over the past decades, some of which have demonstrated extra oil recovery (Blaker *et al*., 2002; Hoefner and Evans, 1995; Martin *et al*., 1992; Norris *et al*., 2014; Ocampo *et al*., 2013; Svorstøl *et al*., 1997). Co-injection and surfactant alternating gas (SAG) injection are two different strategies of foam injection. In the co-injection mode, the gas and the liquid are co-injected at a fixed ratio or foam quality (gas volume fraction of injection fluids), while in the SAG scheme, alternating slugs of surfactant solution and gas are injected into the reservoir. In this paper, SAG injection is considered because it is more favourable on the field scale when foam is applied to provide mobility control due to
(1) improved injectivity upon alternating injection of gas and surfactant solution, and (2) reduced risk of corrosion and risks related to material compatibility because of separate injection of the gas and the liquid (especially in acid- and sour-gas projects) (Farajzadeh *et al*., 2015). The SAG process is similar to water alternating gas process (WAG) and requires little additional effort (Aarra *et al*., 2002; Rossen, 1996; Svorstol *et al*., 1996; Turta and Singhal, 1998; Wellington and Vinegar, 1988).

In oil-free porous media, two foam-flow regimes are identified in the experimental studies of sandpacks by Osterloh and Jante (Alvarez *et al*., 2001; Osterloh and Jante Jr, 1992). In the "low-quality" regime, at high liquid superficial velocity and lower gas superficial velocity, the pressure gradient (∇p) is nearly independent of the liquid flow rate, but depends mainly on the gas flow rate (Alvarez *et al*., 2001; Holt *et al*., 2000; Rossen and Wang, 1999). In other words, the low-quality regime is that at lower superficial velocity of gas and larger velocity of water, in which ∇p contours are nearly horizontal. In the "high-quality" foam regime, at relatively large superficial velocity of gas and small superficial velocity of water, the ∇p contours are nearly vertical. In this regime, the pressure gradient is reasonably independent of the gas flow rate, as predicted by the P_c^* model (Cheng *et al*., 2000; Ma *et al*., 2012). The transition zone between the two regimes was characterized by a specific value of the gas fractional flow f_g (foam quality being gas flowrate divided by the total flowrate), f_g^*.

In order for the foam pilot to be successful, the oil/foam displacement needs to be monitored to establish foam stability and determine how far the foam propagates deep into the reservoir before collapsing. The objective of a foam-flood field trial is usually to investigate whether foam can be generated near the wellbore and be propagated along the reservoir. It is also of desire to determine the characteristics or in-situ rheology of the generated foam. A primary concern is indeed foam generation in typical field velocities far from the injection well and when surfactant and gas travel

through different paths inside the reservoir. Appropriate techniques need to be identified to allow for monitoring the foam stability as well as foam conformance within the reservoir. For this purpose, the deployed monitoring technologies should include measuring of the bottom-hole pressure vs. time, drilling an observation well using to monitor changes in fluid saturations during the foam injection and well logging (e.g. foam generation measurement via RST (reservoir saturation tool) logging).
Pressure-transient test can be conducted to monitor and evaluate the foam injection field trial. A pre-foam pressure fall-off test can be used to determine the initial condition before foam injection (Harpole *et al*., 1994; Kuehne *et al*., 1990). Foam propagation will then be inferred from a series of pressure-transient tests. The fall-off testing can be used to estimate in-situ fluid mobilities at various points during the base line (WAG) and SAG injection periods. In this paper, we investigate the pressure fall-off test data for foam during a SAG process by discussing the dependency of pressure data on foam-model parameters.

Certain foam behaviour (foam formation, stability and distribution) is required to maintain the above-mentioned targets. Pressure fall-Off testing (PFO) is often conducted as one of the cheapest and simplest surveillance techniques to evaluate well performance and injectivity (Abramochkin *et al*., 2009; Mahani *et al*., 2011; Van den Hoek *et al*., 2012). The method monitors the transient pressure in the injection zone during the shut-in period of the injection well for a time sufficient to conduct a valid observation of the pressure fall-off. Reservoir parameters such as effective permeability and skin factor are the primary targets in the well-test analysis.
However, we need to clarify some questions about the foam performance in a reservoir using pressure transient test, e.g.

a) Do we see the foam generation in the formation?
b) How can we capture the changes in foam properties versus time?
c) Can we infer the in-situ rheology of the generated foam in the formation?

During the well-test analysis in a single-phase system, permeability is determined from the stabilized section of the pressure-derivative line from the pressure-derivative log-log plot (Bourdet *et al*., 1983). However, in a two-phase model, the mobility changes between the injected phase and the phase in place is not taken into account by the conventional interpretation approach. The injected fluid with different properties than the fluid in-place creates saturation discontinuities between the region, where the injected fluid predominates, and the region where the original reservoir fluids predominate previously. The injected fluid creates an additional plateau in the pressure derivative log-log curve corresponding to the radial flow due to the injected fluid (e.g. water permeability at S_{orw} in water-injection stage), which is separated from the stabilized radial-flow line created by the oil phase in place due to change in mobility (e.g. effective oil permeability at S_{wi}) and rock wettability (Abramochkin *et al*., 2009). Therefore, it is necessary to consider the injection radius and volume occupied by the injected phase into the formation (Abramochkin *et al*., 2009). Well testing can be done during the base line (WAG without surfactant) and during SAG to collect data for comparing the base line with the foam injection period.

In general, if the radius of investigation of a test does not go beyond the injected fluid bank, the well test result will only yield the formation permeability due to the injected fluid. If the test is long enough to see the oil zone, the changes in permeability within the shut-in time will be seen. The only permeability values obtained from PFO after a reasonable period of time of injection is the permeability of the injected fluid flooded zone at the residual oil saturation (Falade *et al*., 1996). The slope of the first straight line segment that develops on a standard plot of pressure versus logarithm time is commonly used to determine the mobility of the first zone (Merrill Jr *et al*., 1974). The slopes of the straight line segments beyond the first one have also been used to estimate the properties of other zone.

Foam has a non-Newtonian nature, which is reflected in viscosity dependence on the flow, leading to shear-thinning (or sometimes shear-thickening) behaviour in the low-quality regime. The shear-thinning behaviour can have an important effect on the pressure response in the PFO test. In general,

for shear-thinning fluids, the effective viscosity can be obtained by a power law: $\mu = K\gamma^{n-1}$, in which μ is the effective viscosity, K is the consistency index, Υ is shear rate and n is flow behaviour index. For Newtonian fluids, $n=1$, whereas for a shear thinning fluid, $n<1$.

Some analytical and numerical models have been carried out to study the effect of the transient nature of the non-Newtonian (shear thinning) fluids in well testing in the literature (Ikoku, 1979; Katime-Meindl and Tiab, 2001; Lund and Ikoku, 1981; Mahani *et al.*, 2011; Odeh and Yang, 1979; Vongvuthipornchai and Raghavan, 1987). Partial differential equation for a power-law fluid flow through porous media was derived (Odeh and Yang, 1979) by relating the viscosity to the shear rate (Savins, 1969). Non-Newtonian fluids, unlike the Newtonian fluids which show the horizontal pressure derivative log-log curve during radial flow, exhibit an inclined curve. It was shown that the infinite-acting pressure derivative is more inclined when the flow-behaviour index decreases (Katime-Meindl and Tiab, 2001).

It is the purpose of this paper to investigate the pressure and pressure-derivative curve to interpret the pressure data in reservoirs flooded by foam during a SAG process. First the pressure and pressure-derivative behaviour in respect to the foam injection around well bore are shown, and then the foam front and propagation in contact with initial oil in place are investigated. The STARS foam model is used to simulate the foam behaviour in the reservoir. Sensitivity analysis of foam parameters (*epdry*, *fmdry* and *epcap*), foam generation, stability and shear-thinning behaviour is expected to be obtained by pressure transient test behaviour. It is anticipated that pressure vs. time plots of transient data reflect the change in mobility with a slope change.

Foam behavior - implicit-texture (IT) foam model

Design of a foam-injection project requires understanding and controlling of foam behaviour in the reservoir. There are several models for foam flow through porous media in literature, which includes models with explicit relations for foam generation and destruction (population balance models) and models with implicit relations to track the foam texture (Afsharpoor *et al.*, 2010; Bertin *et al.*, 1998; Chang *et al.*, 1990; Chen *et al.*, 2010; Cheng *et al.*, 2000; CMG, 2011; Ettinger and Radke, 1992; Falls *et al.*, 1988; Friedmann *et al.*, 1991; Islam and Ali, 1988; Kam and Rossen, 2003; Kovscek *et al.*, 2010; Li *et al.*, 2006; Martinsen and Vassenden, 1999; Namdar Zanganeh and Rossen, 2013; Rossen *et al.*, 1999; Vassenden and Holt, 2000; Zhou and Rossen, 1995; Zitha and Du, 2010).
We used local equilibrium or implicit texture (Lotfollahi *et al.*, 1999) foam model, i.e., that of the STARS simulator (Cheng *et al.*, 2000; CMG, 2011; Martinsen and Vassenden, 1999). This model scales the gas mobility by a function, FM, when foam is present:

$$\lambda_g^f = \lambda_g^{nf}.FM = \frac{\lambda_g^{nf}}{1 + fmmob\prod_{i=1}^{n} F_i} \tag{2}$$

where λ_g is the gas mobility and superscripts ^{f} and ^{nf} represent the cases with and without foam respectively. Parameter *fmmob* is the maximum (or reference) mobility reduction factor that could be achieved by foam when all conditions are favorable. The "F_i" functions in Eq. (2) reflect the effects of different physical parameters such as surfactant concentration, water saturation, oil saturation (and composition), capillary number, etc., on foam behavior in porous media. In this paper we focus on the dry-out and shear-thinning functions. The dry-out effect means that the mobility of gas increases enormously near the injection well, leading to greatly increase of injectivity. The dry-out function is defined in STARS as

$$F_w = 0.5 + \frac{1}{\pi}\arctan\left(epdry\left(S_w - fmdry\right)\right) \tag{3}$$

Parameter *fmdry* is the water saturation at which foam experiences significant coalescence and consequently in the limit of large *epdry* it is equivalent to S_w^*. Parameter *epdry* controls the sharpness of transition from the high-quality regime to the low-quality regime: when *epdry* is very large the transition is sharp and foam collapses within a very narrow range of water saturation. When *epdry* approaches infinity foam coalescence occurs at a single water saturation (S_w^*). In the most recent version of STARS, the parameter *fmdry* is renamed *sfdry*, and *epdry* is renamed *sfbet* (Coombe *et al.*,

2012). In that model *sfdry* can be represented as a function of surfactant concentration, oil saturation, salt concentration, and capillary number. If one disables these other functionalities *sfdry* is a constant and plays the same roll as *fmdry* does above.
The shear-thinning function is defined as

$$F_{shear} = \begin{cases} 1 & N_{Ca}\left(=\frac{k\nabla P}{\sigma}\right) < fmcap \\ \left(\frac{fmcap}{N_{Ca}}\right)^{epcap} & N_{Ca}\left(=\frac{k\nabla P}{\sigma}\right) > fmcap \end{cases} \quad (4)$$

where∇P is the magnitude of pressure gradient, k is permeability, and σ is the gas-water surface tension under reservoir conditions. Parameter *fmcap* should be set to the smallest capillary number expected to be encountered by foam in the simulation (Boeije and Rossen, 2013; Cheng *et al*., 2000), and *epcap* represents the extent of shear-thinning behavior. Newtonian behavior corresponds to *epcap* = 0 and positive *epcap* to shear-thinning behavior.
In this paper, we plot gas fraction vs. apparent viscosity of foam μ_{app}, which can be easily calculated by Eq. 5.

$$\mu_{app} = \frac{k\nabla p}{u_t} \quad (5)$$

where k is the permeability and u_t is total superficial velocity.

Radial Simulation Model

We study a two-dimensional homogenous cylindrical model with a height and radius of 30 m and 300 m respectively by generating the horizontal expanding grid in the radial direction with small grid blocks near the well (< 1m) to investigate the effect of foam parameters during the pressure fall-off test (see Figure 1). The medium is initially filled with oil and connate water, i.e., no gas is initially present in the system. We consider a vertical injection well at the center of the model with a constant pressure boundary (at 300 m distance of the well), assuming the injected fluid front moves radially outwards pushing the oil ahead of it. The wellbore-storage effect is ignored in this model and the well is presented as an instantaneously reacting system. The simulation has been set up and run using Shell's dynamic in-house modular reservoir simulator MoReS for reservoir and fluid properties listed in
Table ***1***. In addition, a relative-permeability model for a three phase system was generated using Corey correlation with the parameters listed in
Table ***1*** and equation presented in Appendix A.
The water and gas injection rates are set to 100 m^3/day to keep the injection pressure below the formation fracture pressure. Pressure fall-off test is included in the simulation following two days of water injection and ten days of gas injection. The period of fall-off test was five days. The rheology of the foam was modelled by implicit-texture (IT) foam model, as described in the previous section. The effect of oil saturation on foam behaviour is neglected in this paper.

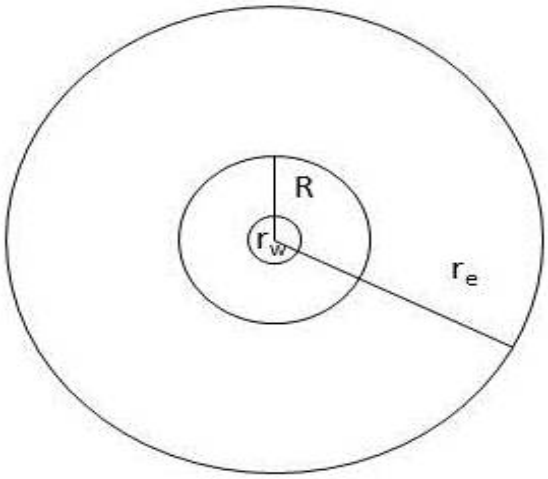

Figure 1 *Radial composite model for the fall-off test analysis, r_w is wellbore radius, R is the radius of invaded zone and r_e is the reservoir radius.*

Table 1 *Reservoir and fluid prpoperties in reservoir simulation.*

Porosity	0.21	Gas compressibility	1.68×10^{-3} bar^{-1}
Well bore radius	0.1 m	Injection rate	100 m^3/d
External radius	300 m	Connate water saturation	0.1
Horizontal permeability	100 mD	Residual oil saturation	0.3
Vertical permeability	10 mD	Residual gas saturation	0
Formation thickness	30 m	n_w	4
Initial pressure	200 bar	n_g	1.8
Oil and water viscosity	1 cp	Water compressibility	3×10^{-6} psi^{-1}
Gas viscosity	0.02 cp	Oil compressibility	1.4×10^{-5} psi^{-1}

Results and discussion

This radial model allows alteration of the mobility due to the injection of a given fluid (e.g. water and gas) into a reservoir saturated initially with oil. To be able to see the different radial flow related to each phase, first we consider 12 days of water injection in a reservoir saturated with 90% oil followed by a 5-day shut-in period.

In Figure 2, two radial flows are identified. As the time elapses the pressure derivative reflects fluid mobility difference at increasing distances from the injection well. The level of the flat trend (radial flow) in the log-log curve is inversely proportional to the fluid mobility (μ/kh) at the corresponding distance from the injector. The early flat trend is related to the mobility of the injected water, while the later trend corresponds to the mobility of the oil bank. As the viscosity of oil and water is considered equal in this paper, the ratio of the mobility in the inner zone (water) to mobility in the outer zone (oil) corresponds to the ratio of relative permeability values of each phase at the corresponding saturation. The constant pressure boundary (at 300 m distance of the well) leads to a decrease of the derivative towards zero.

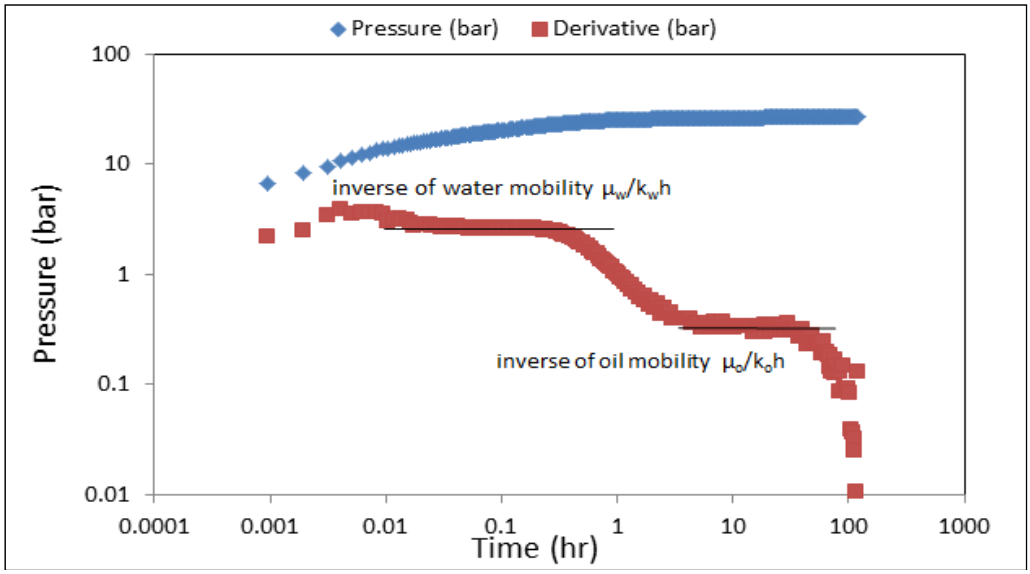

Figure 2 *Simulated pressure fall-off test after 12 days of water injection.*

We also consider 12 days of only gas injection in a reservoir initially filled with 90% oil followed by 5 days of fall-off test. In Figure 3, the first stabilized horizontal slope of radial flow corresponds to the effective permeability of the gas, whereas the second one shows the permeability of the oil in place. Due to its higher mobility, the derivative of the pressure in the log-log plot is lower compared to that of the oil. Comparing Figure 2 and Figure 3 reveals that gas would not sweep the reservoir in a piston-like manner, as expected due its high mobility.

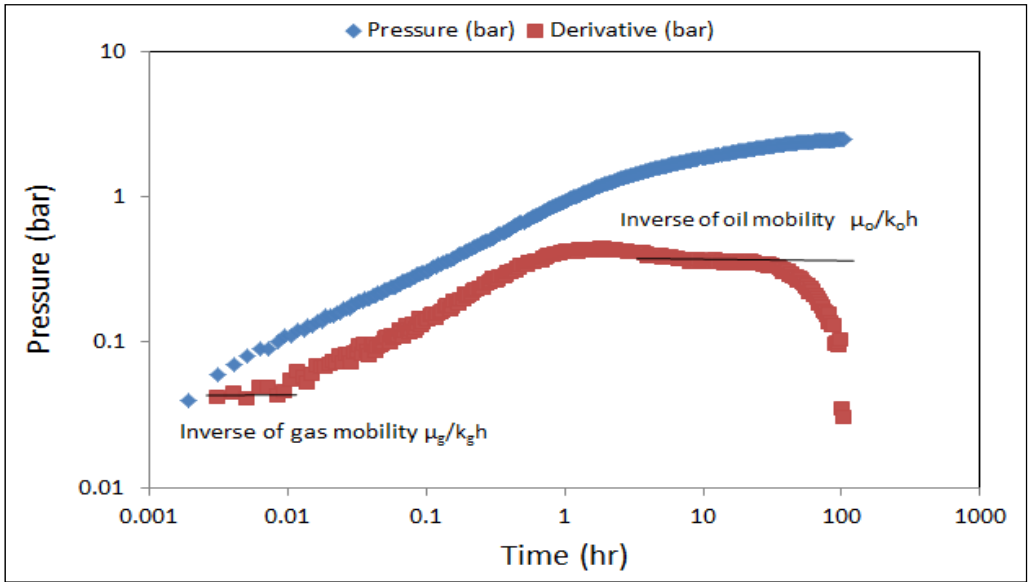

Figure 3 *Simulated pressure fall-off test after 12 days of gas injection.*

We compute type curves for the foam injection PFO test to study the impact of the following parameters in eqs. (3) and (4): 1) *epdry*, 2) *fmdry*, and 3) *epcap*.

A) Effect of *epdry*

The objective of this section is to show the effect of different values of *epdry* (10-10000) in the PFO behaviour for surfactant alternating gas (SAG) floods, while other foam parameters are kept constant (*fmmob*= 8975, *fmdry*=0.3 and *epcap*=0). In the IT foam model, *epdry* determines the sharpness of the transition from a high-quality to a low-quality foam regime, as depicted in Figure 4. In the SAG-injection process, *epdry* determines the mobility of the fluid behind the foam front. Foam mobility

increases from displacement front towards the injector. When the value of *epdry* is small, this transition is more gradual and it is possible that the mobility of foam at the injector is comparable or even lower than the mobility of the foam at the front. When the value of *epdry* is large, this transition is more abrupt and for very large values of *epdry* the foam mobility at the injector could be much higher than the front. This is shown for the foam parameters used in this paper in Figure 4. The mobility of the fluids close to the injector (or even from injector towards the displacement front) imposes the injectivity, and therefore it is of importance to infer the *epdry* value from the pressure fall-off analysis in field applications of the foam.

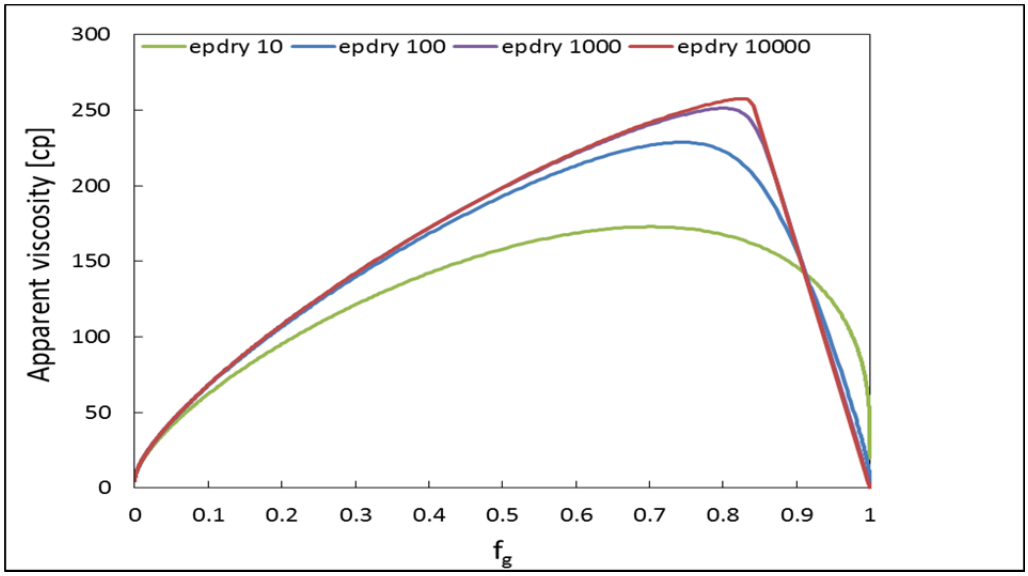

Figure 4 *Effect of epdry on foam behavior based on IT model excluding the capillary number dependent function in low quality regime (fmmob= 8975, fmdry=0.3 and epcap=0).*

The effect of *epdry* on the pressure and its derivative is shown on Figure 5 and Figure 6, respectively. For the sake of comparison we have included the pressure fall-off results for a WAG process. The duration of water and gas injection for the WAG case is the same as those of the SAG process. The pressure-derivative behavior reflects the fluid mobility values at different values of *epdry* at increasing distance from the well. The pressure and derivative curve during and after the SAG process imply that the increased level (black lines in Figure 6) is attributed to in-situ foam generation. As shown in Figure 6, the radial flow flat line for *epdry* =10 has the highest level in log-log curve, which means that foam has the lowest mobility leading to stronger foam due to slower dry-out. This is also confirmed by viscosity profiles corresponding to different values of *epdry* in Figure 4. Following the radial flow flat trend for foam, small stabilized trend is related to the injected water (see also Figure 2), whereas the oil radial flow stabilization is masked by boundary effects. The apparent viscosity and gas saturation vs. distance from the injection well is shown in Figure 7. The apparent viscosity in this paper is calculated from $\frac{\mu_g}{FM}$ (note the difference with eq. (5)). Lower values of *epdry* lead to higher viscosity in the foam bank and more piston like displacement of the foam. As shown in Figure 6, extended radial flow trend for lower values of *epdry* can be due to the lower mobility of the foam extended from the front towards the injector.

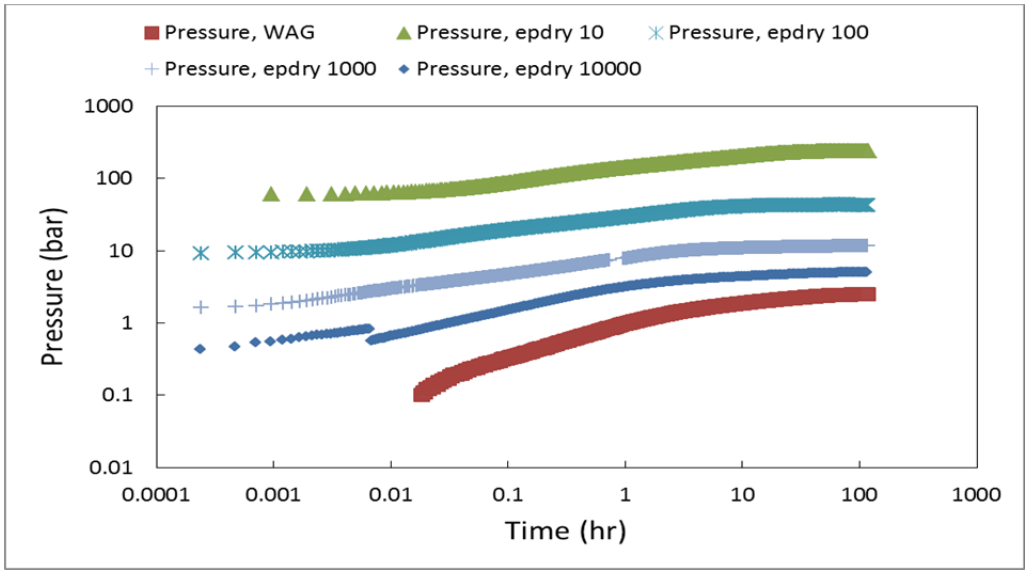

Figure 5 *Effect of epdry on simulated pressure in log-log plot vs. shut-in time in surfactant alternating gas flooding, be noted that the capillary number dependent function is excluded in low quality regime (fmmob= 8975, fmdry=0.3 and epcap=0).*

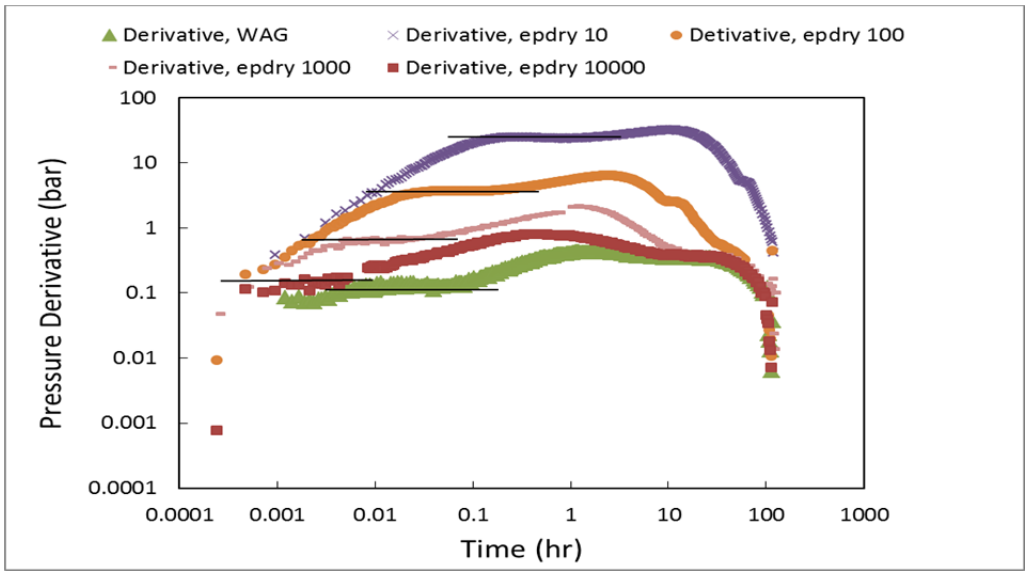

Figure 6 *Effect of epdry on simulated pressure derivative in log-log plot vs. shut-in time in surfactant alternating gas flooding, be noted that the capillary number dependent function is excluded in low quality regime (fmmob= 8975, fmdry=0.3 and epcap=0).*

At a higher value of *epdry* (=10000), foam has higher mobility close to the injector and therefore the foam-stabilized radial flow line is close to that of the WAG injection, where there is no foam in-situ. From Figure 6, in the case of *epdry*=1000 and 10000, the first horizontal trend is related to the mobility of the foam (between 0.004 – 0.01 hrs for *epdry* 10000 and between 0.006 – 0.03 hrs for *epdry* 1000), and the second visible horizontal trend (between 10 – 35 hrs) corresponds to the oil in place, from which the reservoir horizontal permeability can be calculated by $k = (70.6 \times q \times \mu \times B)/(h \times Derivative)$. In our model the calculated reservoir permeability is 99.58 mD. Finally the effect of a constant pressure boundary (at 300 m distance of the well) is seen, leading to a decrease of the derivative towards zero. If one compares the levels of foam-stabilized radial flow in Figure 6, the mobility of foam increases 180, 30, 3, and 2 times relative to reference gas mobility for *epdry* values of 10, 100, 1000 and 10000.

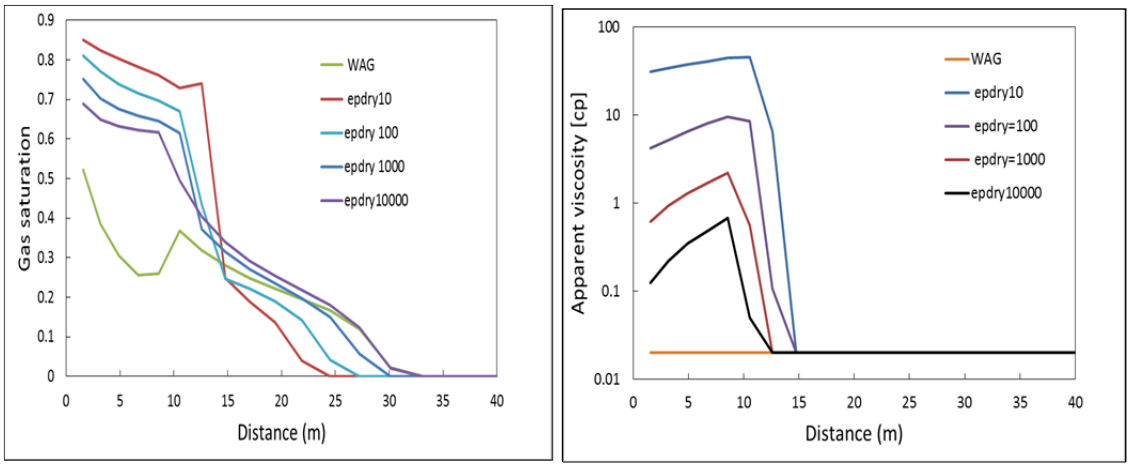

Figure 7 *a) Gas saturation profile for different values of epdry in the top of the reservoir b) Apparent viscosity vs. distance from well for different values of epdry in the top of the reservoir after 12 days of injection.*

We also run the simulation for different values of *epdry* when the reservoir is fully saturated with water. This is to distinguish two-phase flow case from oil-tolerant foam where three-phase flow exists. As one can see in Figure 8, the horizontal trend of the radial flow of foam is similar to the case in which the reservoir is initially saturated with 90% oil. However, the following stabilized radial flow curve is related to the initial water in place, when the reservoir is fully saturated with water, and corresponds to initial oil, when the reservoir contains oil. The difference between the radial-flow level of the oil and water is due to the different relative permeabilities. As shown in Figure 9, when there is no oil in place, the gas saturation along the reservoir does not change significantly with different values of *epdry*.

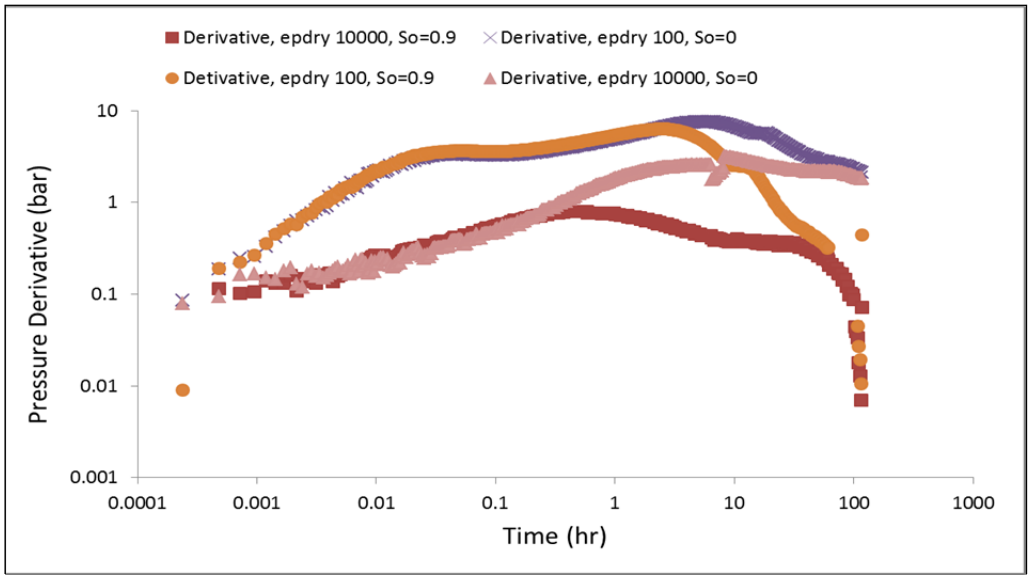

Figure 8 *Effect of epdry on simulated pressure derivative in log-log plot vs. shut-in time in surfactant alternating gas flooding when there is no oil in the reservoir (S_{wi}=1), be noted that the capillary number dependent function is excluded in low quality regime (fmmob= 8975, fmdry=0.3 and epcap=0).*

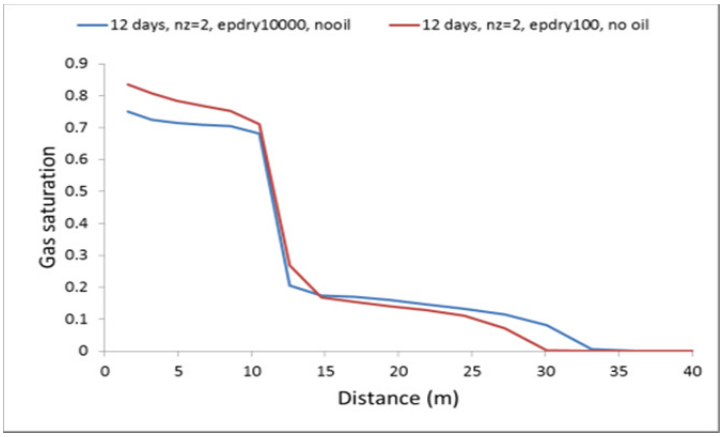

Figure 9 *Gas saturation profile in the top of the reservoir after 12 days of injection for different values of epdry when there is no oil in the reservoir (S_{wi}=1).*

A-1) Larger value of *epdry*

In this section we compare the behavior of foam with a large value of *epdry* =100000 during a SAG process. As shown in Figure 10, foam with large values of *epdry* acts like gas, but later at the front of the foam (the beginning of transition zone pressure derivative at 0.03 hrs) the mobility of foam increases. Although there is no mobility control behind the foam front, at the front there is reasonably low mobility, which can be captured by the PFO test (see Figure 10). This behavior is also confirmed by Figure 11b, in which the apparent viscosity is close to the gas viscosity, and increases as the foam bank moves along the reservoir. This subject has been studied by Farajzedeh *et al*. 2015, who showed relative permeability of foam vs. radius for *epdry*=100000, *fmdry*=0.29 and S_{wc}=0.2. As shown in both figures, foam dries out behind the shock front along the reservoir and consequently the total mobility increases to very high values near the injection well.

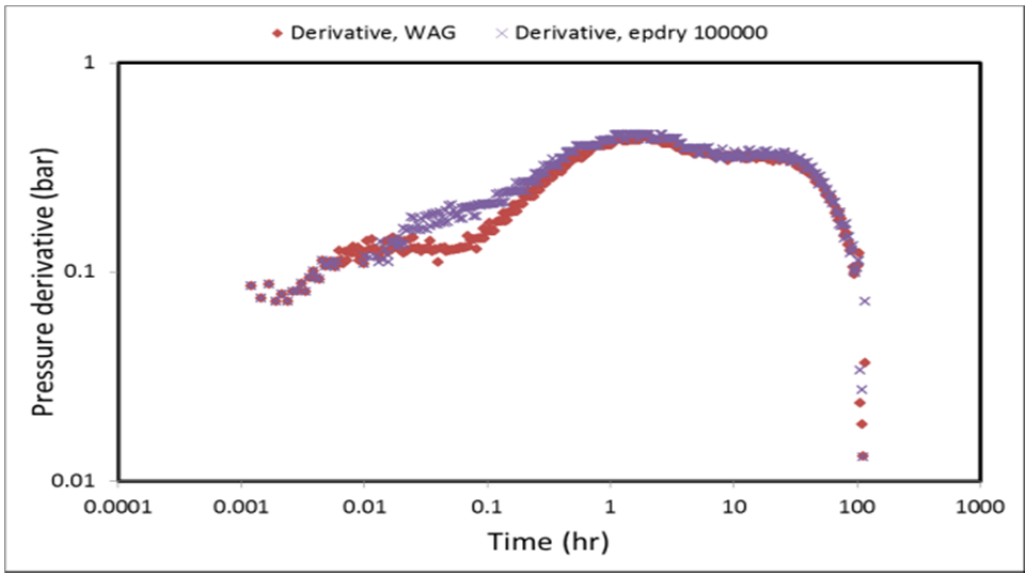

Figure 10 *Effect of large values of epdry (100000) on simulated pressure derivative in log-log plot vs. shut-in time in surfactant alternating gas flooding (fmmob= 8975, fmdry=0.3 and epcap=0).*

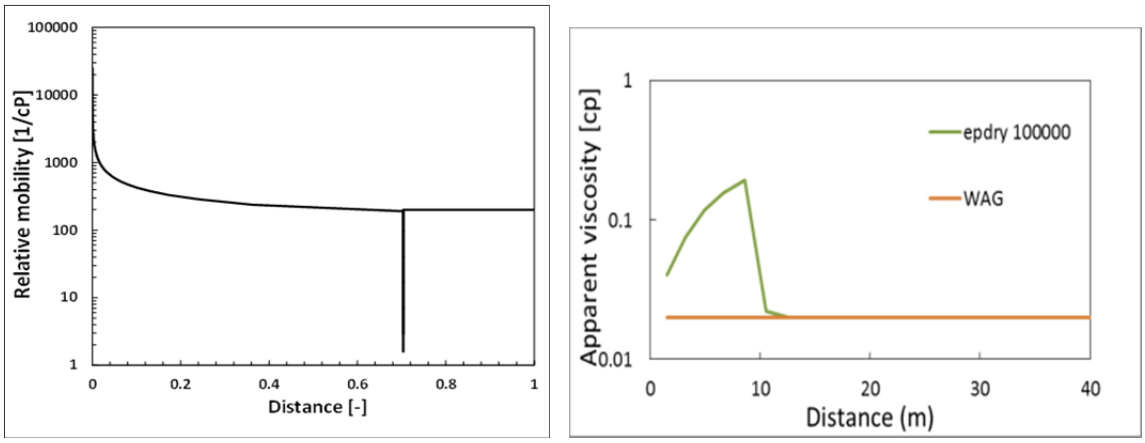

Figure 11 *a) Relative mobility profile after 0.5pv of gas injection into medium fully saturated with surfactant solution(Farajzadeh et al., 2015) b) apparent viscosity vs. distance from well for higher value of epdry in the top of the reservoir after 12 days of injection.*

B) Effect of *fmdry*

It has been experimentally observed that foam experiences an abrupt coalescence when the capillary pressure in the porous medium approaches a certain value referred to as the "limiting capillary pressure", P_c^* (Khatib *et al*., 1988). *fmdry* represents the water saturation corresponding to the P_c^* (also called S_w^*) in the IT foam model. In other words, *fmdry* is the water saturation at or close to the transition water saturation from "low-quality regime" to the "high-quality regime," where foam dry-out dominates the behavior. F_2 in eq. (3) approaches 1 when S_w is much greater than *fmdry* (Martinsen and Vassenden, 1999). Water saturation influences foam mobility in the reservoir, especially when the water saturation is close to the critical water saturation *fmdry*. When the water saturation is close to the critical water saturation *fmdry* (S_w^*), foam begins to collapse. Choosing *fmdry* value very close to irreducible water saturation in reservoir means that the transition foam quality is close to 1 (see Figure 12). We set different values for critical water saturation *fmdry*, below that expected anywhere in the foam bank, but well above the irreducible water saturation. For large values of *epdry*, F_2 changes very dramatically over a small difference in water saturation in the region around the critical water saturation *fmdry*.

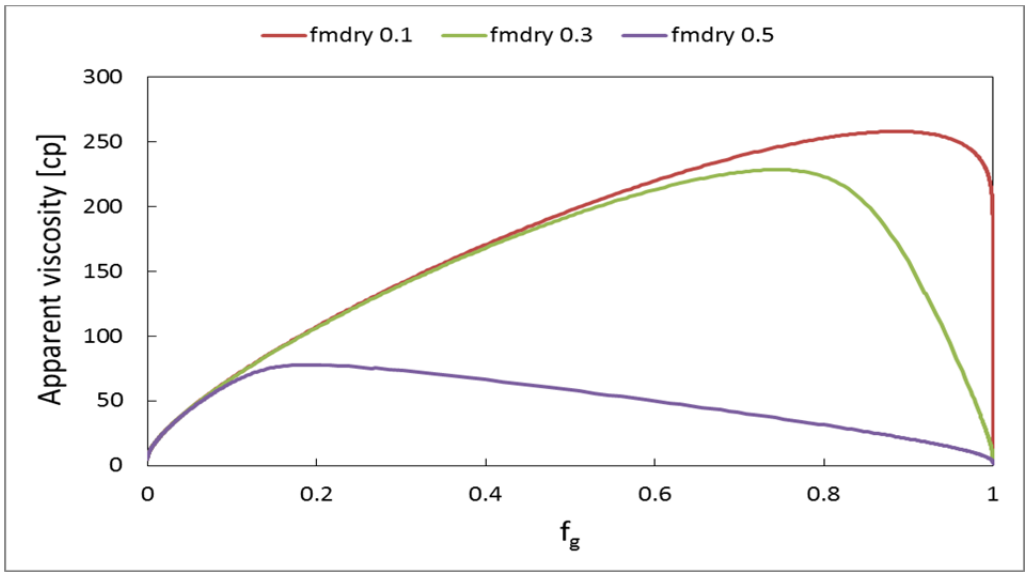

Figure 12 *Effect of fmdry on foam behavior based on LE model excluding the capillary number dependent function in low quality regime (epdry=100, epcap=0, n_w=4 and fmmob= 8975).*

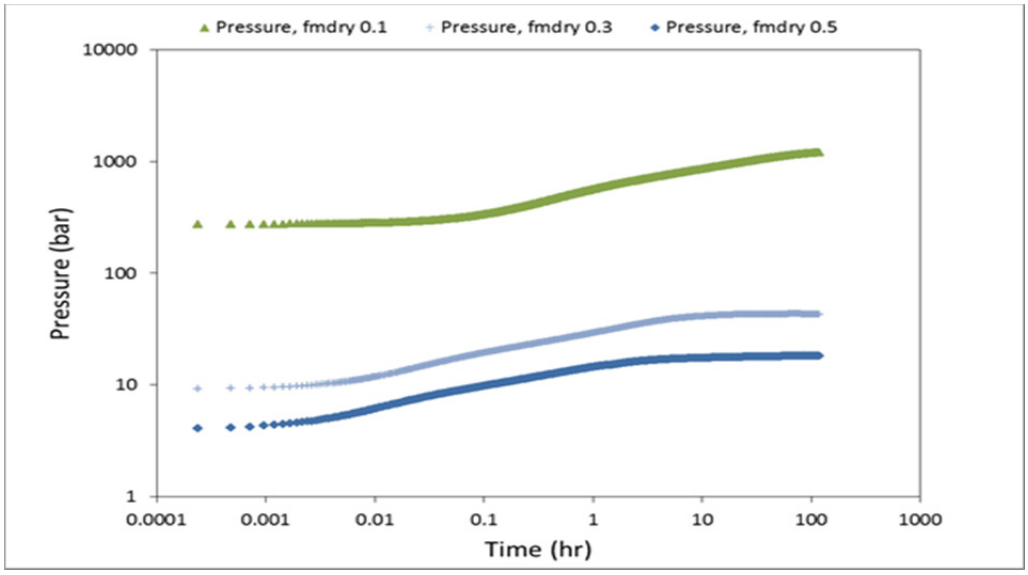

Figure 13 *Effect of fmdry on simulated pressure in log-log plot vs. shut-in time in surfactant alternating gas flooding, be noted that the capillary number dependent function is excluded in low quality regime, (epdry=100, epcap=0, and fmmob= 8975).*

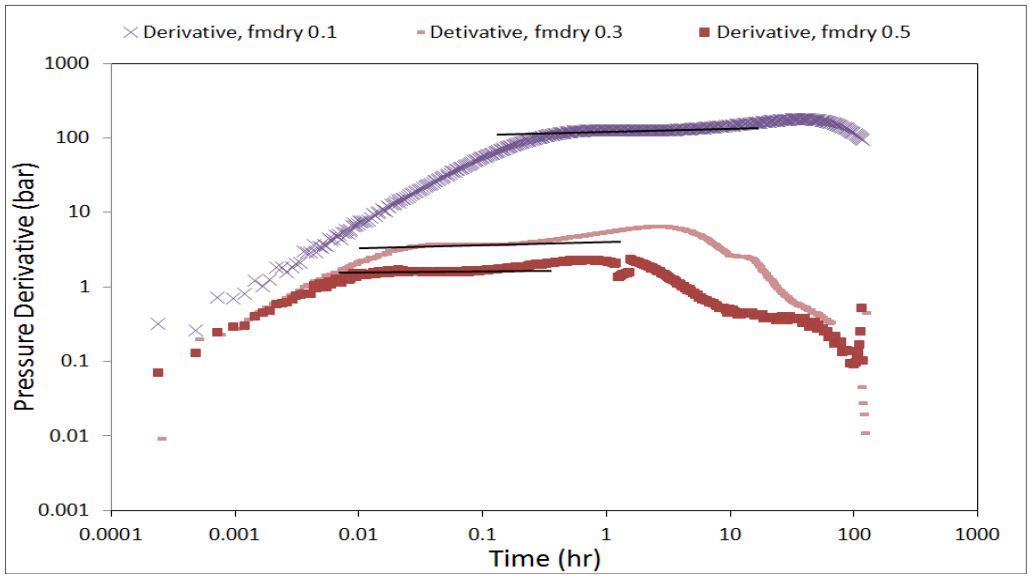

Figure 14 *Effect of epdry on simulated pressure derivative in log-log plot vs. shut-in time in surfactant alternating gas flooding, be noted that the capillary number dependent function is excluded in low quality regime, (epdry=100, epcap=0, and fmmob= 8975).*

As shown in Figure 13 and Figure 14, *fmdry* of 0.1 leads to a higher pressure and pressure derivative stabilized plateau, because this value is always well below the water saturations found in the foam bank. In Figure 15, the viscosity of foam with *fmdry*= 0.1 gives a higher apparent viscosity and collapsed later than the other values of *fmdry*, because the water saturation is not below *fmdry* value until 17 m away from the injection well. For *fmdry*=0.5, the foam collapses closer to the injection well, as the water saturation falls below S_w=0.5 in the override zone about 11 m from the injection well. This is also confirmed with the pressure derivative curve, which shows the first horizontal line as the foam radial flow, then the transition zone between injected fluid and oil in place, then the radial flow related to oil and finally the constant pressure boundary. Whereas *fmdry*= 0.1 does not allow foam to break so easily in the override zone, therefore the only radial flow corresponds to the foam in Figure 14.

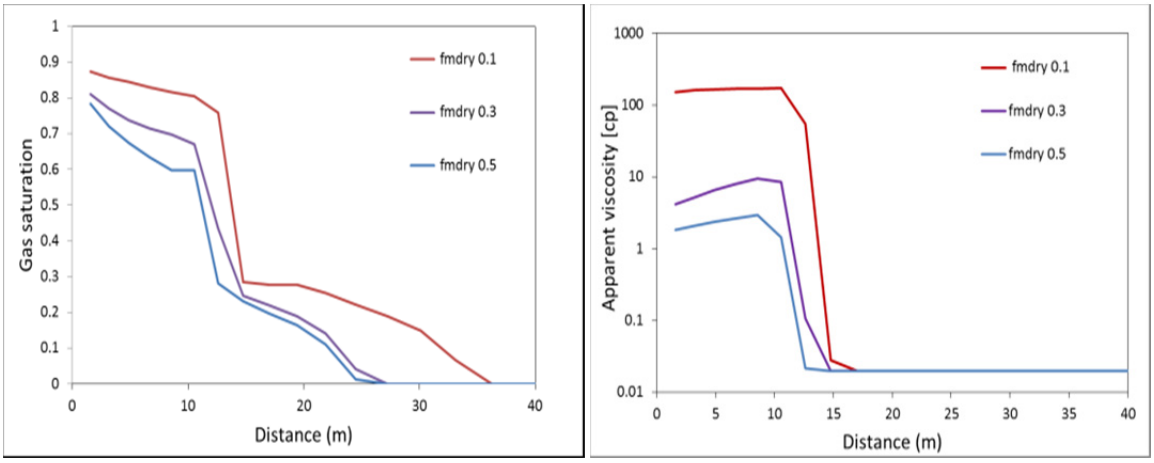

Figure 15 *a) gas saturation profile for different values of fmdry in the top of the reservoir b)apparent viscosity vs. distance from well for different values of fmdry in the top of the reservoir after 12 days of injection.*

C) Effect of *epcap*

At low-quality regime and shear rates encountered under reservoir conditions (0.1-10 s^{-1}), foam typically exhibit shear thinning behaviour captured by *epcap* in the IT foam model. During the injection period, the flow rate varies with distance from the injection well and this will lead to a variation in shear rates. Due to the shear-thinning effect, the apparent viscosity has the lowest value at/around wellbore, and gradually increases with increasing distance from the injector (see Figure 12). Foam gets weaker as the pressure gradient increases if *epcap* > 0. Therefore, because our goal is to represent shear-thinning flow throughout the foam bank, we set *fmcap* to a value less than the smallest value of N_{Ca} expected to be encountered in a simulation. That further implies that the "reference velocity" at which *fmmob* is determined corresponds to this value of N_{Ca}. If foam experiments are conducted in the laboratory at larger value of N_{Ca} encountered in the field, *fmcap* should be the smallest value expected in the simulations and *fmmob* should be extrapolated to that value of *fmcap*.

Figure 17 and Figure 18 show the logarithmic pressure and pressure derivative vs. shut-in time as function of *epcap (epdry*=10, *fmdry*=0.3, and *fmmob*= 8975). When *epcap*=0, foam shows Newtonian behaviour (power-law index n=1), which is confirmed by horizontal stabilization indicating radial formation flow of injected foam between t= 0.1-2 hours. Note that wellbore-storage effect is neglected in this paper. For higher values of *epcap*, foam shows a non-Newtonian behaviour (*n<1*). The logarithmic pressure derivative increases linearly with a slop of *(1-n)/(3-n)* as obtained in the well test analysis of non-Newtonian power-law fluids (Katime-Meindl and Tiab, 2001; Vongvuthipornchai and Raghavan, 1987). The flow behaviour index *n* can be estimated from a PFO test. For Newtonian behaviour (*epcap*=0, *n*=1), radial flow in the reservoir is characterised by a horizontal slope of the pressure derivative, whereas for non-Newtonian behaviour (*epcap*>0, *n*<1), the radial flow is increasing linearly in logarithmic pressure derivative, until the time that the foam front is seen by the PFO test (2 hours). Then the radial flow related to the injected water is shown by the stabilized horizontal slope, and finally the effect of a constant-pressure boundary (at 300 m distance of the well) is seen. This leads to decrease of the derivative towards zero. We estimate the flow behaviour index *n* from the slope of this straight line, resulting to *n*=0.43-0.89 for *epcap*=0.2-1 (see Figure 20).

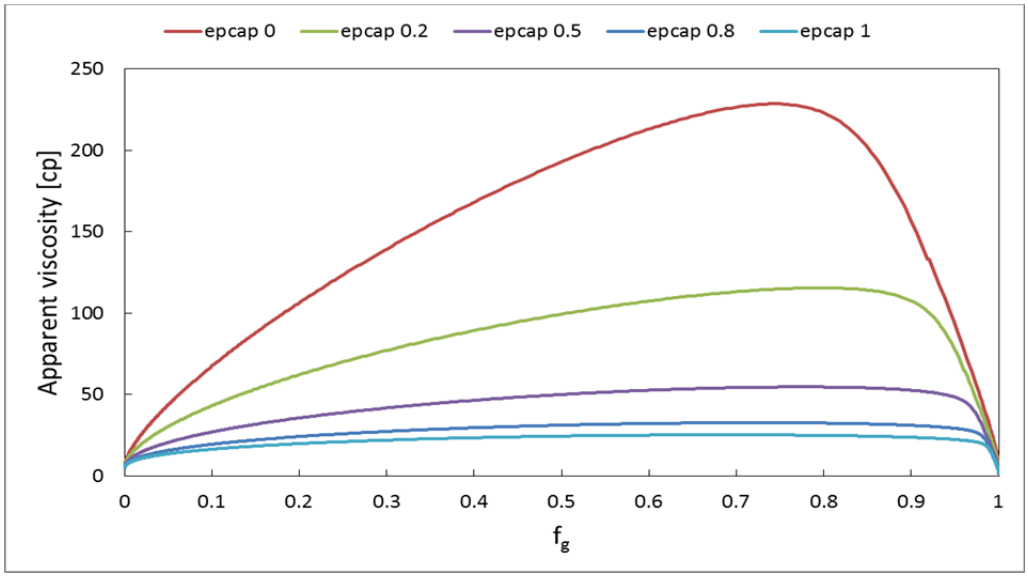

Figure 16 *Effect of epcap on foam behavior based on LE model, (epdry=10, fmdry=0.3, and fmmob= 8975).*

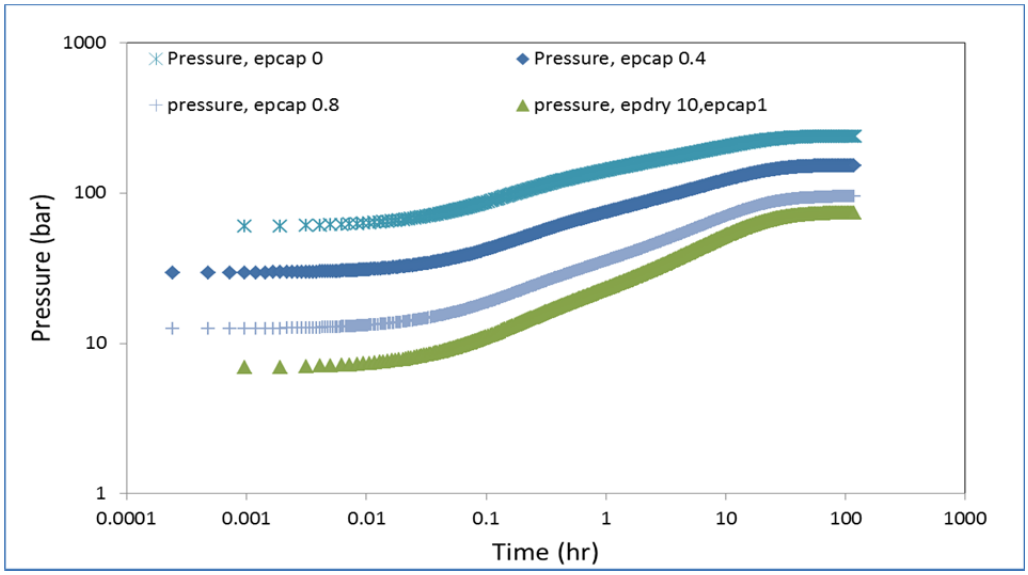

Figure 17 *Effect of epcap on simulated pressure in log-log plot vs. shut-in time in surfactant alternating gas flooding, (epdry=10, fmdry=0.3, and fmmob= 8975).*

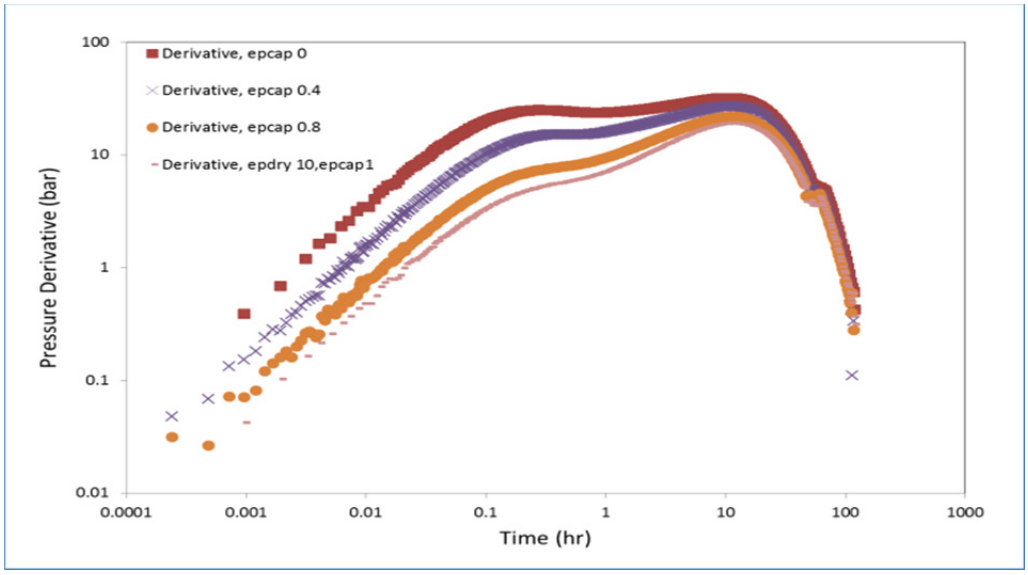

Figure 18 *Effect of epcap on simulated pressure derivative in log-log plot vs. shut-in time in surfactant alternating gas flooding, (epdry=10, fmdry=0.3, and fmmob= 8975).*

In Figure 19, the gas-saturation profile for different values of *epcap* is similar, leading to a closer transition zone between foam and water in Figure 18.

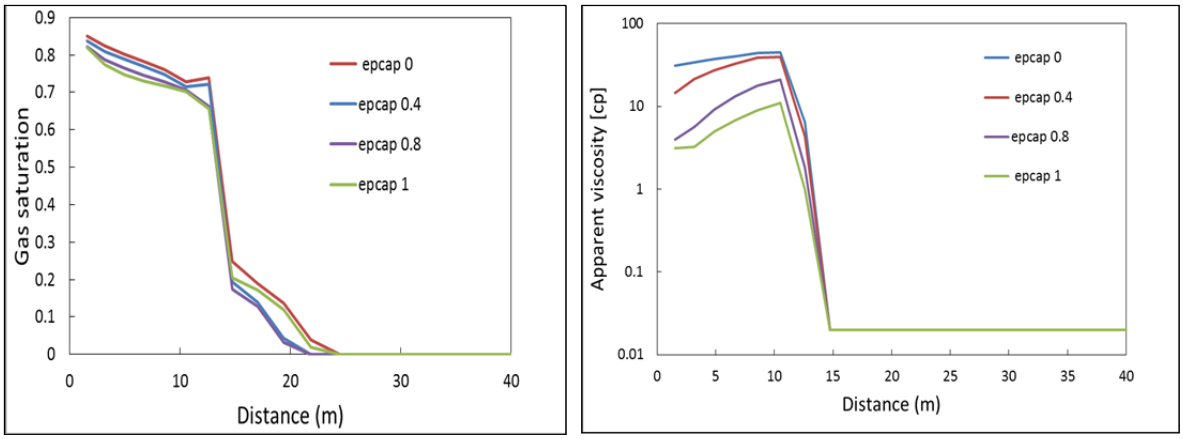

Figure 19 *a) Gas saturation profile for different values of epdry in the top of the reservoir, b) Apparent viscosity vs. distance from well for different values of epcap in the top of the reservoir.*

The relation between *epcap* and the conventional power-law index *n* is obtained considering a bundle-of-tubes for rock, where the rock consists of N uniform, parallel and cylindrical tubes of same radius, leading to the same permeability and porosity of the rock (Bird, 2002). The relation between n and *epcap* based on bundle-of-tubes model ($n = \frac{1}{1+epcap}$) is not exact (Bird, 2002; Shen, 2006). This relation is compared with the values of *n* obtained from the slop of the pressure derivative log -log plot (see Figure 20).

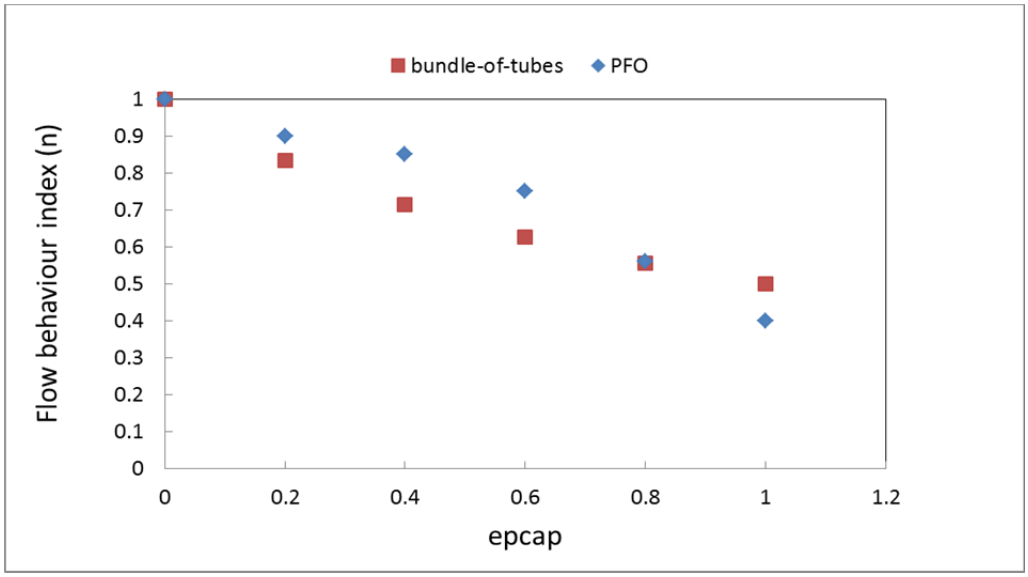

Figure 20 *Flow behavior index variation vs. epcap.*

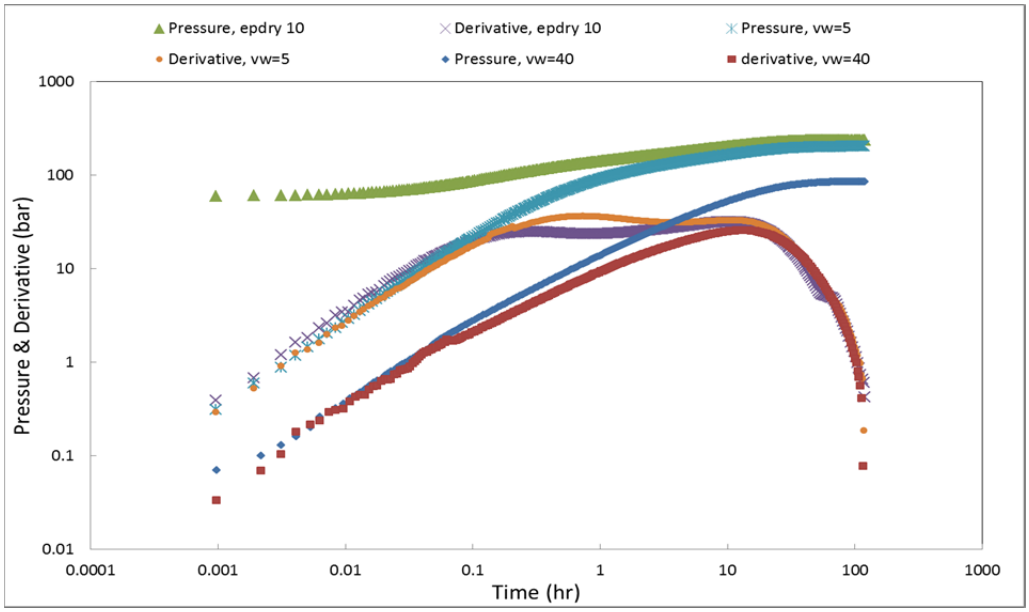

Figure 21 *Impact of wellbore storage on PFO behavior for foam with epdry=10, "small" storage: V_{well}=5 m^3 and "large" storage: V_{well}=40 m^3.*

D) Well-bore storage effect

In this section, we further studied the impact of different wellbore volumes (V_w = 5 m^3 and 40 m^3) on the PFO analysis of foam injection (SAG process) with two values of *epdry* =10 and 1000. As shown in Figures 21 and 22, wellbore storage effect is exhibited by the unit slop part of the PFO derivative curve. For both cases (*epdry* =10 and 1000), it can be seen that the PFO response at short shut-in time is characterized by storage flow-dominated. Wellbore storage masks the foam radial flow part which is characterized by horizontal line in the figure. This is particularly pronounced in the presence of larger storage. One can see when the wellbore storage increases, the pressure and pressure derivative curves move in the log-log plot to the right. If the reservoir boundary is far away or more injection fluid bank is injected in the reservoir, the foam radial flow can be visible after the wellbore storage effect. However, locating the pressure gauges downhole and measuring of the pressure data at sand face are recommended to avoid the masking of the foam radial flow by wellbore storage or fracture induction.

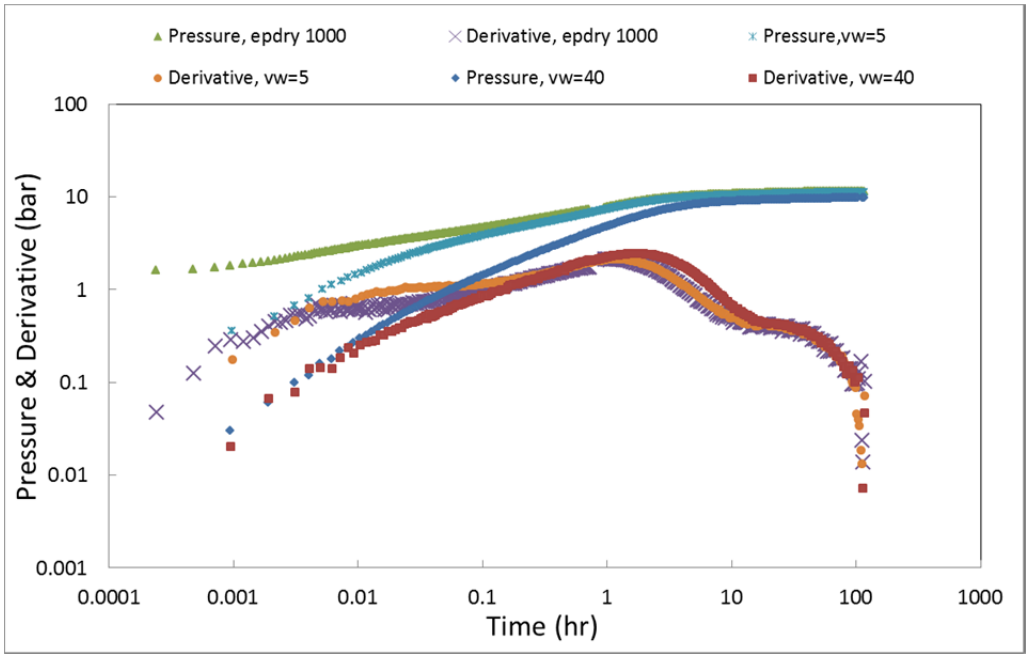

Figure 22 *Impact of wellbore storage on PFO behavior for foam with epdry=1000, "small" storage:* V_{well}*=5* m^3 *and "large" storage:* V_{well}*=40* m^3.

Conclusions

The objective of this study was to determine the effects of different foam-model parameters on the response of the pressure-transient analysis of the pressure fall-off (PFO) test. We used an implicit-texture foam model to simulate foam rheology in the reservoir. In a radial system we simulated a period of water or surfactant injection, which is followed by a gas injection period. Afterwards, the well was shut-in to simulate a pressure fall-off test. The effect of different foam-model parameters such as *epdry, fmdry,* and *epcap* was then studied. We assert that the PFO test can provide valuable information from which foam-model parameters can be estimated under field conditions. The obtained results can then be used to predict the efficiency of foam in enhancing the oil recovery. This model is the first step towards a numerical tool to generate type curves for foam injection, which will be combined by semi-analytical tool in the future as a robust tool.

The surfactant-alternating gas (SAG) process creates two regions in the reservoir, with foam around the wellbore and water or oil away from the well, which yields to two radial flow stabilizations on pressure derivative. The mobility control behind the foam front and at the front can be captured by the PFO test. In the case of non-Newtonian behaviour of foam, the foam radial flow increases linearly in the logarithmic-pressure derivative, until the time that the foam front can be seen by the PFO test. Different values of *epcap* (*epcap*>0) lead to shear thinning behaviour of the foam resulting in flow behaviour index of 0.4<*n*<0.89.

Acknowledgements

We gratefully acknowledge Shell and PETRONAS for funding the project and granting the permission to publish this work. We thank Dr. Tibi Sorop for a careful review of the manuscript.

Appendix A

We assume that the three-phase relative permeability can be calculated using the Corey correlation given below.

$$k_{rw} = K_{rw}\left(\frac{S_w - S_{wc}}{1 - S_{wc} - S_{orw}}\right)^{n_w} \quad \text{(A.1)}$$

$$k_{row} = K_{row}\left(\frac{1 - S_w - S_{orw}}{1 - S_{wc} - S_{orw}}\right)^{n_{ow}}$$

$$k_{rg} = K_{rg}\left(\frac{S_g - S_{gc}}{1 - S_{wc} - S_{gc}}\right)^{n_g}$$

$$k_{rog} = K_{rog}\left(\frac{1 - S_g - S_{org} - S_{wc}}{1 - S_{wc} - S_{org}}\right)^{n_{og}}$$

where,
S_{wc}: Connate water saturation
S_{orw}: Residual oil saturation with respect to water
S_{org}: Residual oil saturation with respect to gas
S_{gc}: Critical gas saturation
K_{rw}: Endpoint water relative permeability
K_{rwg}: Endpoint water relative permeability with respect to gas
K_{row}: Endpoint oil relative permeability
K_{rog}: Endpoint oil relative permeability with respect to gas at critical gas saturation
K_{rgw}: Endpoint gas relative permeability with respect to water at connate water saturation
K_{rg}: Endpoint gas relative permeability
n_w: Corey exponent of water
n_{ow}: Corey exponent of oil with respect to water
n_{og}: Corey exponent of oil with respect to gas
n_g: Corey exponent of gas

References

Aarra, M., Skauge, A. and Martinsen, H. [2002] FAWAG: A Breakthrough for EOR in the North Sea. *SPE Annual Technical Conference and Exhibition*, Society of Petroleum Engineers.

Abramochkin, S., Carnegie, A., Daungkaew, S., Goh, G. and Bee, P. [2009] Water Injection Fall-Off Tests in Deepwater Reservoir: What Do We Actually See Into Formation? *IPTC 2009: International Petroleum Technology Conference.*

Afsharpoor, A., Lee, G. and Kam, S. [2010] Mechanistic simulation of continuous gas injection period during surfactant-alternating-gas (SAG) processes using foam catastrophe theory. *Chemical Engineering Science*, **65**(11), 3615-3631.

Alvarez, J., Rivas, H. and Rossen, W. [2001] Unified model for steady-state foam behavior at high and low foam qualities. *SPE journal*, **6**(3), 325-333.

Andrianov, A., Farajzadeh, R., Mahmoodi Nick, M., Talanana, M. and Zitha, P. [2012] Immiscible foam for enhancing oil recovery: bulk and porous media experiments. *Industrial & Engineering Chemistry Research*, **51**(5), 2214-2226.

Bertin, H., Quintard, M. and Castanier, L. [1998] Development of a bubble-population correlation for foam-flow modeling in porous media. *SPE Journal*, **3**(4), 356-362.

Bird, R.B. [2002] Transport phenomena. *Applied Mechanics Reviews*, **55**(1), R1-R4.

Blaker, T. *et al.* [2002] Foam for gas mobility control in the Snorre field: the FAWAG project. *SPE Reservoir Evaluation & Engineering*, **5**(4), 317-323.

Boeije, C. and Rossen, W. [2013] Fitting foam simulation model parameters to data. *IOR 2013-From Fundamental Science to Deployment*.

Bourdet, D., Whittle, T., Douglas, A. and Pirard, Y. [1983] A new set of type curves simplifies well test analysis. *World Oil*, **196**(6), 95-106.

Chang, S., Owusu, L., French, S. and Kovarik, F. [1990] The Effect of Microscopic Heterogeneity on CO2-Foam Mobility: Part 2-Mechanistic Foam Simulation. *SPE/DOE Enhanced Oil Recovery Symposium*, Society of Petroleum Engineers.

Chen, Q., Gerritsen, M. and Kovscek, A.R. [2010] Improving Steam-Assisted Gravity Drainage Using Mobility Control Foams: Foam Assisted-SAGD (FA-SAGD). *SPE Improved Oil Recovery Symposium*, Society of Petroleum Engineers.

Chen, Y. *et al*., 2013. Switchable Nonionic to Cationic Ethoxylated Amine Surfactants for CO2 Enhanced Oil Recovery in High-Temperature High-Salinity Carbonate Reservoirs. SPE Journal.

Cheng, L., Reme, A., Shan, D., Coombe, D. and Rossen, W., 2000. Simulating foam processes at high and low foam qualities, SPE/DOE Improved Oil Recovery Symposium. Society of Petroleum Engineers.

CMG, 2011. Computer Modeling Group, STARS User's Guide. Calgary, Alberta, Canada.

Coombe, D., Oballa, V. and Buchanan, W., 2012. Foam modelling based on lamella as a dispersed component. report.

Ettinger, R. and Radke, C., 1992. Influence of texture on steady foam flow in berea sandstone. SPE reservoir engineering, 7(1): 83-90.

Falade, G., Namba, T. and El-Hadidi, S., 1996. Analysis of Pressure Fall-off Tests in High Capacity Water Injection Wells, Abu Dhabi International Petroleum Exhibition and Conference. Society of Petroleum Engineers.

Falls, A. *et al*. [1988] Development of a mechanistic foam simulator: the population balance and generation by snap-off. *SPE reservoir engineering*, **3**(03), 884-892.

Farajzadeh, R., Andrianov, A., Krastev, R., Hirasaki, G.J. and Rossen, W.R. [2012] Foam–oil interaction in porous media: implications for foam assisted enhanced oil recovery. *Advances in colloid and interface science*, **183**, 1-13.

Farajzadeh, R. *et al*. [2015] Simulation Of Instabilities And Fingering In Surfactant Alternating Gas (SAG) Foam Enhanced Oil Recovery. *SPE Reservoir Simulation Symposium*, Houston, USA.

Friedmann, F., Chen, W. and Gauglitz, P. [1991] Experimental and simulation study of high-temperature foam displacement in porous media. *SPE reservoir engineering*, **6**(1), 37-45.

Harpole, K., Siemers, W. and Gerard, M. [1994] CO2 Foam Field Verification Pilot Test at EVGSAU: Phase IIIC--Reservoir Characterization and Response to Foam Injection. *SPE/DOE Improved Oil Recovery Symposium*, Society of Petroleum Engineers.

Hirasaki, G. [1989] *Supplement to SPE 19505 The Steam-Foam Process--Review of Steam-Foam Process Mechanisms*.

Hirasaki, G. and Lawson, J. [1985] Mechanisms of foam flow in porous media: apparent viscosity in smooth capillaries. *Society of Petroleum Engineers Journal*, **25**(2), 176-190.

Hoefner, M. and Evans, E. [1995] C02 Foam: Results From Four Developmental Field Trials~ 7787.

Holt, T., Vassenden, F. and Ghaderi, A. [2000] Use of foam for flow control of gas. *SPE/DOE Improved Oil Recovery Symposium*, Tulsa, OK, Paper SPE, 1-7.

Ikoku, C.U. [1979] Practical application of Non-Newtonian transient flow analysis. *SPE Annual Technical Conference and Exhibition*, Society of Petroleum Engineers.

Islam, M. and Ali, S. [1988] Numerical simulation of foam flow in porous media. *Annual Technical Meeting*, Petroleum Society of Canada.

Kam, S.I. and Rossen, W. [2003] A model for foam generation in homogeneous media. *SPE Journal*, **8**(4), 417-425.

Katime-Meindl, I. and Tiab, D. [2001] Analysis of pressure transient test of non-newtonian fluids in infinite reservoir and in the presence of a single linear boundary by the direct synthesis technique. *SPE Annual Technical Conference and Exhibition*, Society of Petroleum Engineers.

Khatib, Z., Hirasaki, G. and Falls, A. [1988] Effects of capillary pressure on coalescence and phase mobilities in foams flowing through porous media. *SPE reservoir engineering*, **3**(03), 919-926.

Kovscek, A. and Radke, C. [1994] Fundamentals of foam transport in porous media. *ACS Advances in Chemistry Series*, **242**, 115-164.

Kovscek, A.R., Chen, Q. and Gerritsen, M. [2010] Modeling foam displacement with the local-equilibrium approximation: theory and experimental verification. *SPE Journal*, **15**(1), 171-183.

Kuehne, D.L., Ehman, D.I., Emanuel, A.S. and Magnani, C.F. [1990] Design and evaluation of a nitrogen-foam field trial. *Journal of Petroleum Technology*, **42**(4), 504-512.

Li, B., Hirasaki, G. and Miller, G. [2006] Upscaling of Foam Mobility Control to Three Dimensions. *SPE/DOE Symposium on Improved Oil Recovery*, Society of Petroleum Engineers.

Li, R.F., Yan, W., Liu, S., Hirasaki, G.J. and Miller, C.A. [2010] Foam mobility control for surfactant enhanced oil recovery. *SPE J.*, **15**(4), 934-948.

Lotfollahi, M., Farajzadeh, R., Varavei, A.J., Delshad, M. and Rossen, W. [1999] comparison of population balance and local equilibrium foam models. *Journal of Petroleum science and engineering*.

Lund, O. and Ikoku, C.U. [1981] Pressure transient behavior of non-Newtonian/Newtonian fluid composite reservoirs. *Society of Petroleum Engineers Journal*, **21**(2), 271-280.

Ma, K., Biswal, S.L. and Hirasaki, G.J. [2012] Estimation of Parameters for Simulation of Steady State Foam Flow in Porous Media. *8th Global Congress on Process Safety*, 1-5.

Mahani, H., Sorop, T., Van den Hoek, P., Brooks, A. and Zwaan, M. [2011] Injection Fall-Off Analysis of Polymer Flooding EOR. *SPE Reservoir Characterisation and Simulation Conference and Exhibition*, Society of Petroleum Engineers.

Martin, F. *et al*. [1992] CO2-foam field verification pilot test at EVGSAU injection project phase I: project planning and initial results, SPE/DOE Enhanced Oil Recovery Symposium. *Society of Petroleum Engineers.*

Martinsen, H. and Vassenden, F. [1999] Foam Assisted Water Alternating Gas (FAWAG) Process on Snorre. *10th European Symposium on Improved Oil Recovery*.

Merrill Jr, L., Kazemi, H. and Gogarty, W.B. [1974] Pressure falloff analysis in reservoirs with fluid banks. *Journal of Petroleum Technology*, **26**(7), 809-818.

Namdar Zanganeh, M. and Rossen, W. [2013] Optimization of foam enhanced oil recovery: balancing sweep and injectivity. *SPE Reservoir Evaluation & Engineering*, **16**(1), 51-59.

Norris, S.O. *et al*. [2014] CO2 Foam Pilot in Salt Creek Field, Natrona County, WY: Phase II: Diagnostic Testing and Initial Results. *SPE Annual Technical Conference and Exhibition*, Society of Petroleum Engineers.

Ocampo, A. *et al*. [2013] Successful Foam EOR Pilot in a Mature Volatile Oil Reservoir Under Miscible Gas Injection. *International Petroleum Technology Conference*.

Odeh, A. and Yang, H. [1979] Flow of non-Newtonian power-law fluids through porous media. *Society of Petroleum Engineers Journal*, **19**(3), 155-163.

Osterloh, W. and Jante Jr, M. [1992] Effects of gas and liquid velocity on steady-state foam flow at high temperature. *SPE/DOE Enhanced Oil Recovery Symposium*, Society of Petroleum Engineers.

Ren, G., Zhang, H. and Nguyen, Q.P. [2011] Effect of Surfactant Partitioning Between CO2 and Water on CO2 Mobility Control in Hydrocarbon Reservoirs. *SPE Enhanced Oil Recovery Conference*, Society of Petroleum Engineers.

Rossen, W. [1996] Foams in enhanced oil recovery. *Surfactant Science Series*, 413-464.

Rossen, W. and Wang, M. [1999] Modeling foams for acid diversion. *SPE Journal*, **4**(2), 92-100.

Rossen, W., Zeilinger, S., Shi, J. and Lim, M. [1999] Simplified mechanistic simulation of foam processes in porous media. *SPE Journal*, **4**(3), 279-287.

Savins, J. [1969] Non-Newtonian flow through porous media. *Industrial & Engineering Chemistry*, **61**(10), 18-47.

Schramm, L.L. [1994] *Foams: fundamentals and applications in the petroleum industry*. American Chemical Society Washington, DC, 242.

Shen, C. [2006] *Experimental and simulation study of foam in porous media*.

Simjoo, M., Dong, Y., Andrianov, A., Talanana, M. and Zitha, P. [2013] CT scan study of immiscible foam flow in porous media for enhancing oil recovery. *Industrial & Engineering Chemistry Research*, **52**(18), 6221-6233.

Svorstøl, I., Blaker, T., Tham, M. and Hjellen, A. [1997] A production well foam pilot in the North Sea Snorre field-Application of foam to control premature gas breakthrough. *9th European Symposium on Improved Oil Recovery.*

Svorstol, I., Vassenden, F. and Mannhardt, K. [1996] Laboratory studies for design of a foam pilot in the Snorre field. *SPE/DOE Improved Oil Recovery Symposium*, Society of Petroleum Engineers.

Turta, A. and Singhal, A. [1998] Field Foam Applications in Enhanced Oil Recovery Projects: Screening and Design Aspects. Paper SPE 48895, *International Conference and Exhibition*, Beijing, China, 2-6 November.

Van den Hoek, P. *et al*. [2012] Application of Injection Fall-Off Analysis in Polymer flooding. *SPE Europec/EAGE Annual Conference*, Society of Petroleum Engineers.

Vassenden, F. and Holt, T. [2000] Experimental foundation for relative permeability modeling of foam. *SPE Reservoir Evaluation & Engineering*, **3**(2), 179-185.

Vongvuthipornchai, S. and Raghavan, R. [1987] Well test analysis of data dominated by storage and skin: non-Newtonian power-law fluids. *SPE Formation Evaluation*, **2**(4), 618-628.

Wellington, S. and Vinegar, H. [1988] *Surfactant-induced mobility control for carbon dioxide studied with computerized tomography.*

Zhou, Z. and Rossen, W. [1995] Applying Fractional-Flow Theory to Foam Processes at the "Limiting Capillary Pressure". *SPE Advanced Technology Series*, **3**(1), 154-162.

Zitha, P. and Du, D. [2010] A new stochastic bubble population model for foam flow in porous media. *Transport in Porous Media*, **83**(3), 603-621.